UCRL-51554

ROCK MELT FROM AN UNDERGROUND NUCLEAR EXPLOSION

T. R. Butkovich

March 11, 1974

Prepared for U.S. Atomic Energy Commission under contract No. W-7405-Eng-48

LAWRENCE
LIVERMORE
LABORATORY

University of California/Livermore

Printed in the United States of America
Available from
National Technical Information Service
U.S. Department of Commerce
5285 Port Royal Road
Springfield, Virginia 22151
Price: Printed Copy $___*; Microfiche $0.95

*Pages	NTIS Selling Price
1-50	$4.00
51-150	$5.45
151-325	$7.60
326-500	$10.60
501-1000	$13.60

TID-4500, UC-35
Peaceful Applications
of Explosions

LAWRENCE LIVERMORE LABORATORY
University of California Livermore, California 94550

UCRL-51554

ROCK MELT FROM AN UNDERGROUND NUCLEAR EXPLOSION

T. R. Butkovich

MS. date: March 11, 1974

Contents

Abstract 1
Introduction 1
Technique 2
Discussion of Results 9
References 10

ROCK MELT FROM AN UNDERGROUND NUCLEAR EXPLOSION

Abstract

Knowledge of the deposition of energy with distance around an underground nuclear explosion has significance in predicting chemical processes in the multimineralic rock substance surrounding the explosion. When a nuclear explosion is detonated, the shock wave that emanates from the explosion center does PdV work on the rock substance and deposits energy. Energy deposition due to the passage of the shock wave is determined from hydrodynamic code calculations which keep track of internal energy with distance and time. The energy distribution with distance depends on the compressibility of the rock. Rock of low density and high porosity requires a larger increase in internal energy to shock it to a given pressure than an essentially pore-free dense rock. Interpretation of hydrodynamic code calculations shows that 1000 to 1200 metric tons/kt of melt is produced from dense granite and that two to three times as much melt is produced from dry porous ash-fall tuff. Radiochemical analysis of melt samples recovered from near the shot point tend to confirm these results.

Introduction

Knowledge of the deposition of energy with distance around an underground nuclear explosion has significance in predicting chemical processes in the multimineralic rock substance surrounding the explosion. For example, the amount of noncondensable CO_2 that is liberated from the carbonates present in many rocks is a function of the amount of carbonate in the rock structure and of the quantity of rock heated above the decomposition temperature of the carbonate. Other chemical processes in which CO_2 is liberated can also occur; however, knowledge of the energy distribution is necessary to make reasonable estimates of the amount of CO_2 evolved. The CO_2 acts as a diluent to other gases and raises the cavity pressure.

When a nuclear explosion is detonated, the shock wave that emanates from the explosion center is the primary means by which energy is distributed. The shock wave does PdV work on the rock substance and deposits some energy. Energy deposition due to the passage of the shock wave can be found from hydrodynamic code calculations which keep track of the specific internal energy with distance and time.

One who is familiar with shock Hugoniots for rock and attenuation of the shock wave with distance might expect that the energy distribution for low-density, high-porosity rocks would be different from that for

low-compressibility, high-density, essentially pore-free rock. The low-density rock requires a much larger increase in internal energy to shock it to a given pressure. Also, the shock wave is attenuated much more rapidly for a shot in a low-density rock (Fig. 1). Consequently, it can be expected that more energy is deposited at higher temperatures in a low-density rock.

Previously reported calculations[1] indicate that approximately 70 metric tons/kt is dynamically shock vaporized and an additional 350 metric tons/kt is dynamically shock melted. However, these regions are at a temperature significantly higher than that required to just melt the rock. With a proper heat-transfer mechanism, much more rock could be melted. One can speculate as to what heat-transfer mechanisms are operating. Blow-off of the walls of the cavity during the later part of the cavity expansion and mixing with its high-temperature contents seems likely. Another process is the transfer of heat to the already warm wall through radiation and convection, raising the temperature to the melting point, with the melt running or raining down under the influence of gravity, exposing more material to the hot cavity environment.

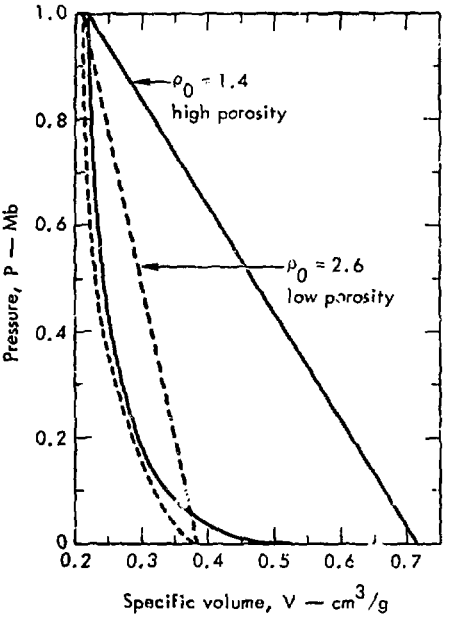

Fig. 1. Typical Hugoniot equations of state for high-density and low-density rocks.

Technique

SOC code calculations for materials of different densities were chosen from those that had previously been made. The shot-point materials were a 1.4-g/cm^3-density, high-porosity rock; a 1.81-g/cm^3, medium-porosity rock; and a 2.61-g/cm^3, low-porosity rock. The Hugoniots for these three rocks are shown in Fig. 2. The calculations were analyzed at late times after cavity growth was complete and the energy all distributed. Heat content was assumed to be the same for all three rocks; the value used was that for granite given by Birch[2] and shown in Fig. 3.

From the energy-vs-scaled-distance relationship obtained from the SOC calculations and the heat-content relationship, a temperature-vs-scaled-distance curve was obtained for each density; these curves are shown in Fig. 4. The

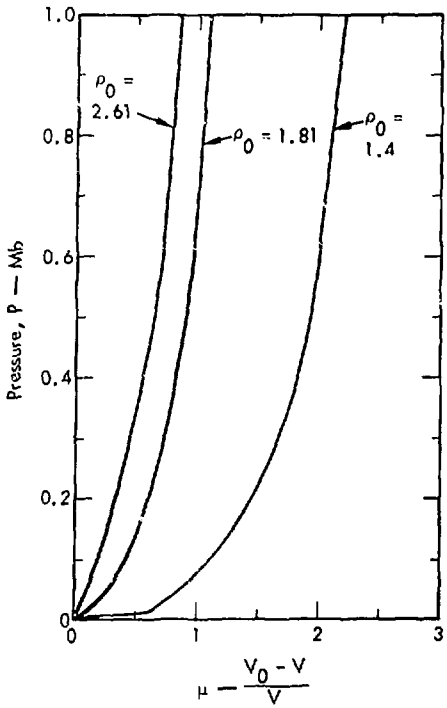

Fig. 2. Hugoniot equations of state used in this study.

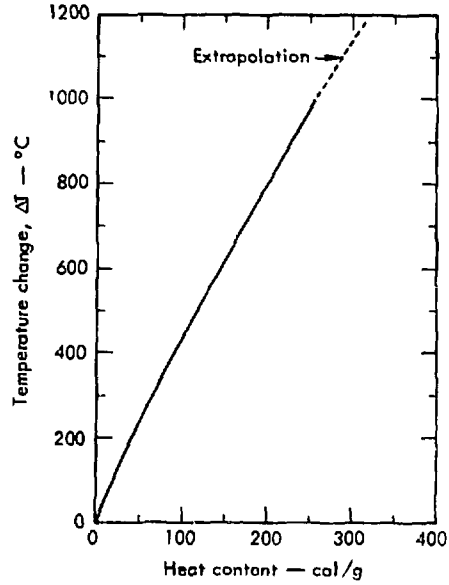

Fig. 3. Heat content of rock as a function of temperature assumed in calculations (taken from Ref. 2).

equation for the straight line on a log-log plot is

$$\Delta T = A \left(\frac{R}{W^{1/3}}\right)^B , \qquad (1)$$

where ΔT is the increase in temperature above ambient in degrees centigrade (ambient is assumed to be 30°C), R is the distance before displacement in meters, and W is the explosion energy in kilotons (10^{12} cal). The constants A and B are the intercept and slope, respectively, of the line. It was also possible to plot the intercepts of the equation against densit and obtain a similar relationship:

$$A = C(\rho)^D ,$$

where ρ is the shot-point density in g/cm^3. For this case

$$A = 8.9 \times 10^5 \, \rho^{-3.156} . \qquad (2)$$

Similarly, the slopes were plotted as a function of density and the relationship

$$B = -4.576 \, \rho^{-0.411} \qquad (3)$$

was obtained. Equation (1) then becomes

$$\Delta T = \frac{8.9 \times 10^5}{\rho^{3.156}} \left(\frac{R}{W^{1/3}}\right)^{\rho^{-4.576}/0.411} . \qquad (4)$$

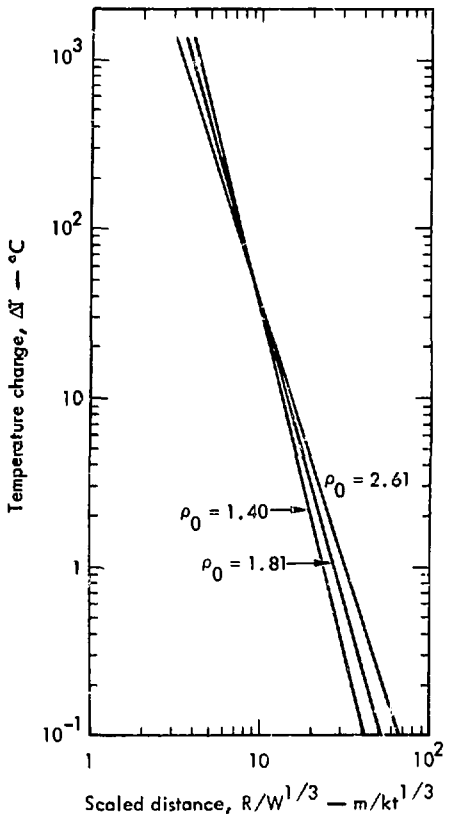

Fig. 4. Shock-induced temperature change as a function of scaled distance for nuclear detonations in rocks of different densities. From Eq. (4).

Table 1 shows the preshot distances for various temperatures and densities calculated from Eq. (4).

To obtain the relationship between the mass M of rock heated to a temperature greater than any ΔT, spherical symmetry was assumed so that

$$M = \frac{4}{3}\pi R^3 \rho.$$

Substituting for R and solving for M, Eq. (4) becomes

$$M = \frac{4}{3}\pi \rho W \left(\frac{\Delta T \rho^{3.156}}{8.9 \times 10^5}\right)^{\frac{-\rho^{0.411}}{1.5253}} . \quad (5)$$

Using Eq. (5), it is possible to obtain the fraction of energy of the explosion between two temperatures. The integral Q gives the total energy deposited:

$$Q = \int_{T_2}^{T_1} E \, dM . \quad (6)$$

The relationship between heat content and temperature from Fig. 2 was approximated by

$$E = \left(\frac{\Delta T}{5.42}\right)^{1.048} . \quad (7)$$

Using Eqs. (5) and (7),

$$Q = \alpha \left(T_1^{\beta} - T_2^{\beta}\right), \quad (8)$$

where

$$\alpha = \left(\frac{4}{3}\pi\rho W\right)\left(\frac{\rho^{3.156}}{8.9 \times 10^5}\right)^{\frac{-\rho^{0.411}}{1.5253}} \times \left(\frac{\rho^{0.411}}{1.5253}\right)\left(\frac{1}{5.42}\right)^{1.048} \times \left(1.048 - \frac{\rho^{0.411}}{1.5253}\right),$$

and

$$\beta = 1.048 - \frac{\rho^{0.411}}{1.5253} .$$

Table 1. Distances for various temperatures and shot-point densities (ρ_0).

Yield (kt)	Distance (m) at temperature						
	1000°C	500°C	300°C	200°C	100°C	10°C	1°C
ρ_0 = 1.4 g/cm^3							
1	4.21	5.01	5.70	6.31	7.50	13.37	23.83
10	9.07	10.80	12.27	13.59	16.17	28.21	51.35
100	19.54	23.26	26.44	29.27	34.83	62.07	110.63
ρ_0 = 2.0 g/cm^3							
1	3.81	4.66	5.40	6.08	7.44	14.51	28.34
10	8.21	10.04	11.64	13.10	16.02	31.28	61.06
100	17.68	21.63	25.08	82.22	34.52	67.79	131.56
ρ_0 = 2.6 g/cm^3							
1	3.39	4.25	5.01	5.71	7.15	15.06	31.73
10	7.71	9.15	10.79	12.31	15.40	32.46	68.73
100	15.75	19.71	23.26	26.52	33.19	69.92	147.29

Figure 5 shows a plot of Eq. (8) in terms of temperature vs fraction of total energy between T_1 = 1000°C and T_2 = 0.01°C. Note that about 25% of the energy is between these two temperatures for the shot-point density ρ = 1.4 g/cm^3, and about 72% of the energy is between these two temperatures for ρ = 2.8 g/cm^3, with a varying fraction between these limits for other densities in this range.

The integration gives the amount of energy at temperatures outside of T_1, which can be considered the melt temperature. By assuming that the energy which is not outside the melt temperature is in the melted rock, the mass of rock melted can be calculated. Table 2 shows the fraction of energy outside the melt calculated from Eq. (8) with various T_1 (melt temperatures) and T_2 = 0.001°C for different shot-point densities. Figure 6

Table 2. Fraction of energy outside of different melt temperatures for different shot-point densities (ρ_0).

ρ_0 (g/cm^3)	Energy fraction at temperature				
	1400°C	1200°C	1000°C	800°C	600°C
1.4	0.2697	0.2555	0.2397	0.2216	0.2006
1.6	0.3315	0.3161	0.2987	0.2787	0.2543
1.8	0.3969	0.3806	0.3621	0.3406	0.3143
2.0	0.4626	0.4459	0.4268	0.4046	0.3775
2.2	0.5414	0.5243	0.5047	0.4817	0.4535
2.4	0.6229	0.6057	0.5861	0.5629	0.5341
2.6	0.7125	0.6956	0.6761	0.6529	0.6240
2.8	0.8121	0.7956	0.7765	0.7536	0.7248

shows the fraction of melt above T_1 (1 minus the values in Table 2).

Table 3 shows the amount of melt calculated as a function of density and assumed melt temperatures by dividing the fraction of energy in the melt by ΔH_{melt}, the enthalpy for melt. ΔH_{melt} values were obtained, by extrapolating the values in Fig. 2, as the specific energy to raise

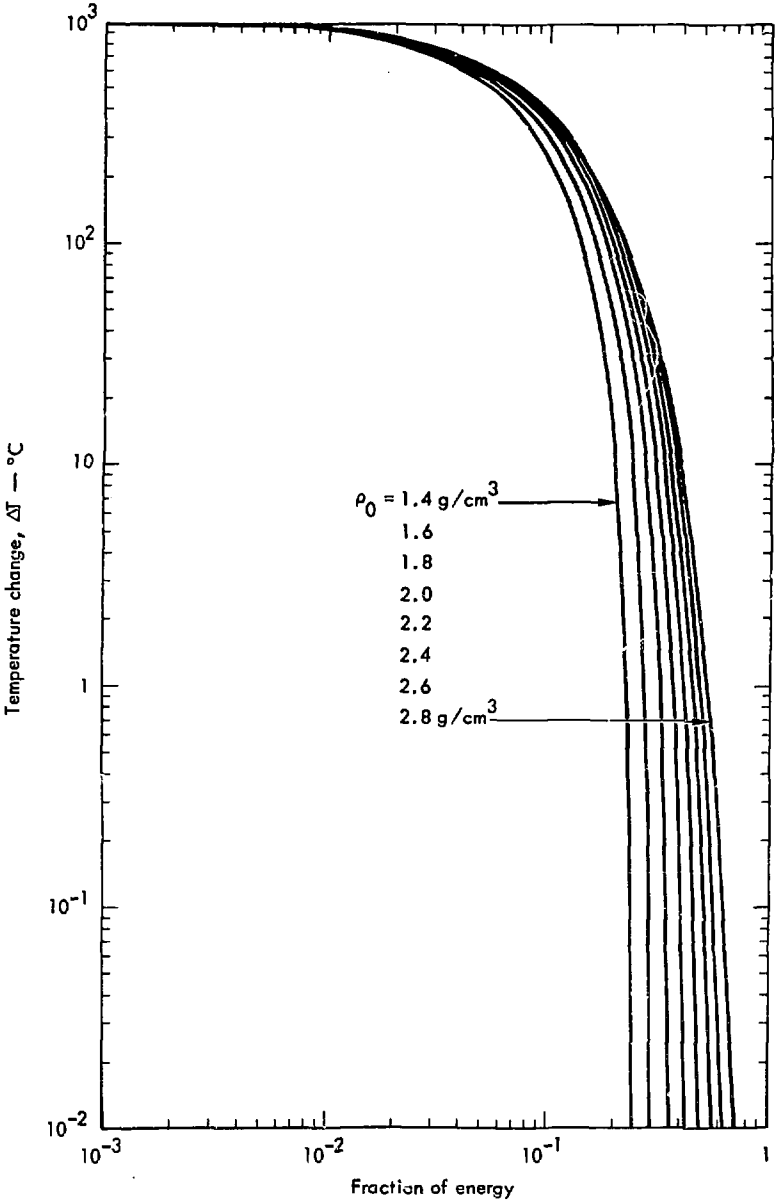

Fig. 5. Fraction of energy in rock between assumed melt temperature of 1000°C and lower temperatures for rocks of different shot-point densities.

Table 3. Mass of rock melted for rocks of different densities (ρ_0) and different assumed melt temperatures and enthalpies (ΔH_{melt}).

	Mass (metric tons $\times 10^9$) at temperature and enthalpy (cal/g)				
ρ_0 (g/cm^3)	1400°C 449	1200°C 393	1000°C 336	800°C 280	600°C 224
1.4	1656	1894	[illegible]	2780	3570
1.6	1489	1770	2087	2576	3327
1.8	1343	1576	1899	2355	3058
2.0	1197	1410	1706	2126	2779
2.2	1021	1210	1474	1851	2445
2.4	840	1003	1232	1561	2080
2.6	640	775	964	1280	1679
2.8	418	520	665	880	1229

the rock to the melt temperature plus the latent heat of fusion, which was assumed to be 80 cal/g.[2]

The calculations show that the amount of rock that is potentially melted by an underground nuclear explosion is a rather strong function of the density of the shot-point material. Fortunately, there are data available to check these results. G. Higgins[3] suggested analyzing the radiochemical data on melt samples recovered from near the explosion center on many nuclear events at the Nevada Test Site. On the basis of experimental measurements, it is generally assumed that all refractory nuclides are associated with the melt.[4] Melt puddle samples are recovered in postshot drilling and analyzed in the laboratory as to the fraction of activity of various refractory isotopes produced by the nuclear explosion. If one assumes that the melt is perfectly mixed and the samples are representative of all the melt, then the amount of melt produced per kiloton can be obtained. Six to fourteen puddle samples are measured for each event, and the fractions of activity for a number of different refractory isotopes are obtained. For the present study, radiochemistry data were analyzed for about 40 events; however, shot-point densities are available for only about half of these.

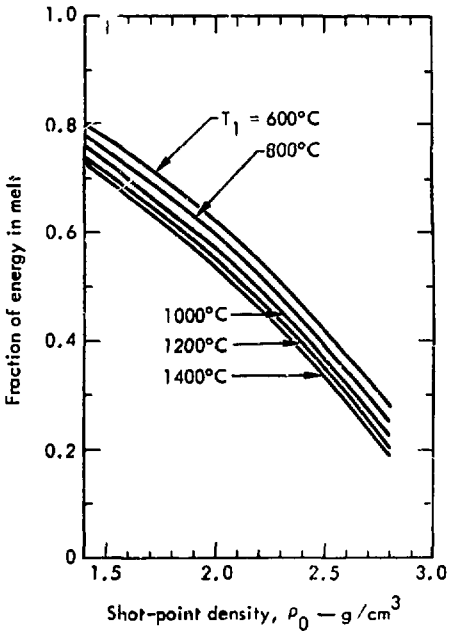

Fig. 6. Fraction of energy in rock melt vs shot-point density assuming different melt temperatures.

There is considerable scatter in the results of the measurements. Figure 7 shows the amount of melt per kiloton of yield vs shot-point density. The points were obtained by averaging the radiochemical measurements on puddle-glass samples. The standard deviation is about 50% of the average values shown. There is some question of whether the radiochemical samples are representative of the puddle glass; sample descriptions indicate that some contain impurities such as water and drilling mud. One would then expect that those samples that were

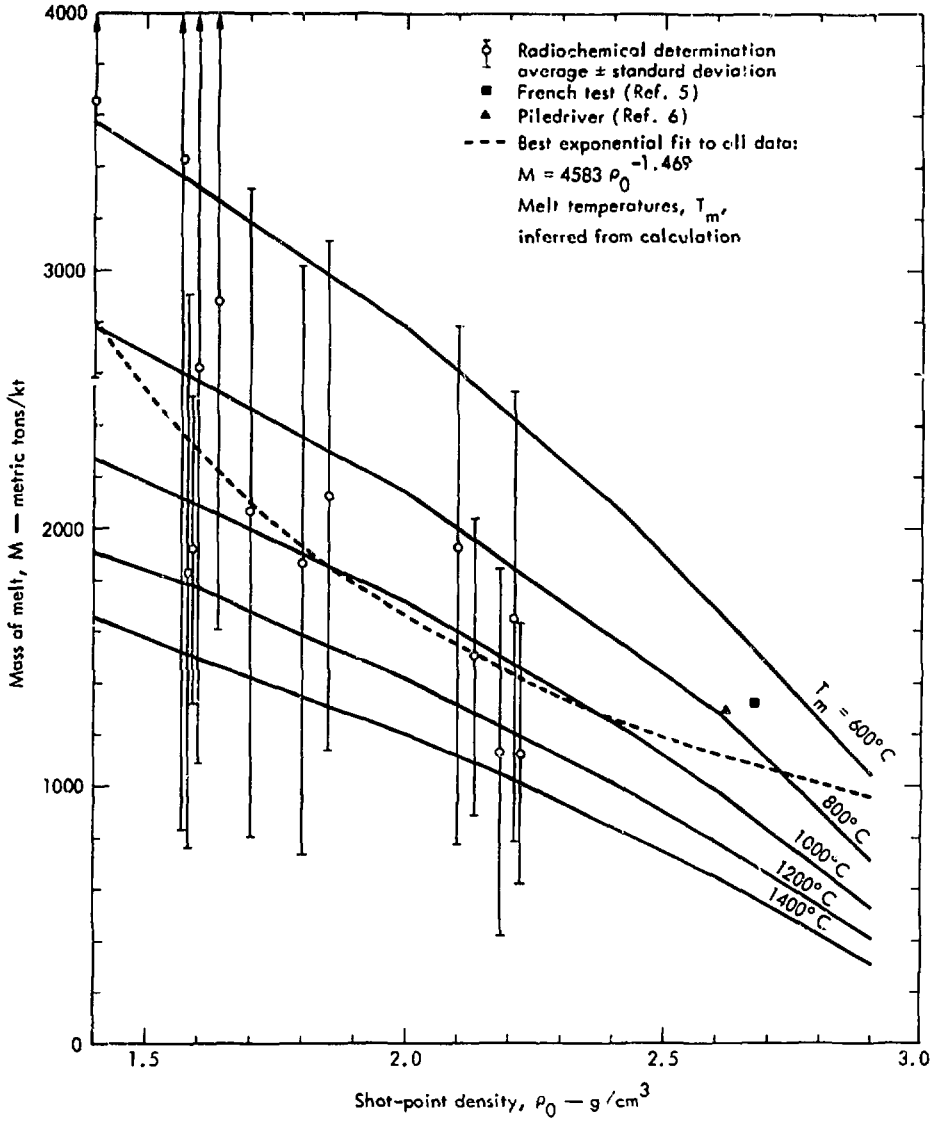

Fig. 7. Calculated amount of melt per kiloton vs shot-point density assuming different melt temperatures. Mean values from radiochemical determinations are shown for LLL data along with their standard deviations. Direct determinations from a French test and from the Piledriver Event are also shown.

indicated to contain impurities would consistently give higher values for amount of melt. However, if these differences exist, they are hidden in the scatter of the data. Two additional data points obtained by other techniques are also shown. Cohen[5] shows values obtained in a granite in which the French underground tests were conducted, and Borg[6] obtained an amount of melt for the Piledriver Event, also in granite. Figure 7 also shows the exponential best fits to the data, along with melt temperatures inferred from calculations given in Table 3.

Discussion of Results

In an underground nuclear explosion, the total amount of rock melt produced dynamically by the shock wave and by the redistribution of the excess heat appears to be a function of the shot-point density. This result is obtained calculationally, and it is supported by experimental evidence. Although there is a large scatter in the radiochemical results, there is a definite trend toward more melt produced in lower-density (higher porosity) shot-point media. The large scatter of the radiochemical results can be attributed in part to the sampling techniques, whereby considerable impurities are included in the melt samples. The total melt produced appears to range between about 1300 metric tons/kt of energy yield for the high-density, low-porosity shot-point rocks to two to three times this amount for the low-density, high-porosity shot-point rocks.

The water content of the shot-point rock was not taken into consideration either in the calculations or in estimating a melt temperature for shots in which radiochemical data were available. Water content has two important effects: The first is that increasing water content tends to depress the melting temperature of the rock.[7] The other is that an increased water content increases the heat content of the rock, since the average specific heat of the water component of the rock is about five times greater than that of the solid component.

References

1. T. R. Butkovich, Gas Equation of State of Natural Materials, Lawrence Livermore Laboratory, Rept. UCRL-14729 (January 1967).
2. F. P. Birch, Ed., Handbook of Physical Constants, GSA Special Paper No. 36 (1942).
3. G. Higgins, Lawrence Livermore Laboratory, private communication.
4. H. A. Tewes, H. B. Levy, and L. L. Schwartz, Nuclear Chemical Copper Mining Radiological Considerations, Lawrence Livermore Laboratory (to be published).
5. P. Cohen, Gases Formed in an Underground Nuclear Explosion: Chemical Equilibria and Potential Application, Lawrence Livermore Laboratory, Rept. UCRL-Trans-10616-3 (1972) (translation of IAEA-PL-388/7, pp. 199-209, 1970).
6. I. Y. Borg, Long-Lived Radionuclides Contained in Glasses Produced by Nuclear Explosion in Granodiorite (Piledriver Event), Lawrence Livermore Laboratory, Rept. UCRL-74588 (1972).
7. A. J. Piwinskii and R. F. Martin, "An Experimental Study of Equilibrium with Granite Rocks at 10 kb," Contrib. Mineral. Petrol. 29, 1 (1970).